Dissecting the Determinants of Cyclin-Dependent Kinase 2 and Cyclin-Dependent Kinase 4 Inhibitor Selectivity†

David J. Pratt,‡,△ Jo Bentley,⊥ Philip Jewsbury,§ F. Tom Boyle,§ Jane A. Endicott,‡ and Martin E. M. Noble*,‡

Laboratory of Molecular Biophysics, Department of Biochemistry, University of Oxford, South Parks Road, Oxford, OX1 3QU, UK, Northern Institute for Cancer Research, Paul O'Gorman Building Medical School, University of Newcastle, Framlington Place, Newcastle, NE2 4HH, UK, and AstraZeneca, Mereside, Alderley Park, Macclesfield, Cheshire, SK10 4TG, UK

Received February 24, 2006

Cyclin dependent kinases are a key family of kinases involved in cell cycle regulation and are an attractive target for cancer chemotherapy. The roles of four residues of the cyclin-dependent kinase active site in inhibitor selectivity were investigated by producing cyclin-dependent kinase 2 mutants bearing equivalent cyclin-dependent kinase 4 residues, namely F82H, L83V, H84D, and K89T. Assay of the mutants with a cyclin-dependent kinase 4-selective bisanilinopyrimidine shows that the K89T mutation is primarily responsible for the selectivity of this compound. Use of the cyclin-dependent kinase 2-selective 6-cyclohexylmethoxy-2-(4′-sulfamoylanilino)purine (NU6102) shows that K89T has no role in the selectivity, while the remaining three mutations have a cumulative influence. The results indicate that certain residues that are not frequently considered in structure-aided kinase inhibitor design have an important role to play.

Introduction

Passage through the eukaryotic cell cycle is controlled by the sequential activation of members of the cyclin-dependent protein kinase (CDK[a]) family. A hallmark of a cell's progression to a cancerous state is the assimilation of mutations within the genes encoding either selected members of this family or proteins that directly or indirectly regulate their activities. In particular, the cyclin D−CDK4−INK4−pRB axis is central to G1 progress,[1] and is altered in the majority of human cancers.[2,3] For example, levels of cyclin D1 are commonly elevated in many neoplasms including breast tumors, colorectal, head and neck carcinomas and lung cell tumors,[4] and mutations within the INK4a (CDK2N2A) gene have been repeatedly documented in various human melanomas.[5]

CDK2 is extensively regulated through association with cyclins A and E, the inhibitory proteins $p21^{Cip1}$ and $p27^{Kip1}$ and by phosphorylation.[6] Cyclin E overexpression and depression of $p27^{Kip1}$ activity are the two most common alterations to the network of CDK2 regulation observed in tumors of diverse origin.[4,7,8] In some cancers, notably breast, cyclin E levels correlate with patient survival and can be used as a prognostic indicator.[9] Genetic alterations within the *p27* gene are rare, and posttranslational processing of the protein seems to be the major cause of down-regulation.[10]

The up-regulation of CDK2 or CDK4 activity in different tumor types suggests that CDK2- or CDK4-selective inhibitors would be useful chemotherapeutics. Structure-aided design approaches have benefited from the relative ease with which CDK2 can be crystallized and have contributed to the rapid development of CDK2 inhibitors.[11] In contrast, CDK4 has proved resistant to crystallization, hindering a proper assessment of the structure−activity relationships of the CDK4 inhibitors developed to date. To overcome this lack of structural information, other methods, including the use of CDK2 as a surrogate kinase,[12] homology modeling,[13] and mutagenesis[14] have been used.

Here, the roles of four nonconserved residues in CDK2/CDK4 inhibitor selectivity have been studied using site-directed mutagenesis and X-ray crystallographic structure determination.

Results and Discussion

Residues Implicated in Defining CDK2/CDK4 Inhibitor Selectivity. Analysis of the structures of CDK2 bound to eight chemically distinct ligands identified 33 residues that lie within 5 Å of one or more of the ligands (Figure 1). The equivalent CDK4 residues are ∼70% identical (22 of 32). The nonconserved residues correspond to the following CDK2 mutations: E8A, K9E, E12V, T14A, F82H, L83V, H84D, K89T, Q131E, and L133I. The side-chain of Phe82 defines part of the 'top' of the ATP adenine-binding site; the backbone of Leu83 forms hydrogen bonds with all the ligands studied, and the side-chain defines part of the 'bottom' of the adenine site; and the side-chain of Lys89 lies at the 'entrance' of the ATP binding site. These nonconserved residues were hence considered potential prime determinants of CDK inhibitor selectivity and were mutated in CDK2 to produce CDK4-like mutants. His84 was additionally mutated due to its proximity to Leu83.

CDK2 mutants were constructed to assay the influence of the chosen residues on inhibitor selectivity. The initial aim of producing the quadruple mutant $CDK2^{F82H/L83V/H84D/K89T}$ was achieved via the single mutant $CDK2^{K89T}$ and triple mutant $CDK2^{F82H/L83V/H84D}$. Two further mutants were then constructed based on preliminary assay of $CDK2^{F82H/L83V/H84D}$, namely $CDK2^{F82H}$ and $CDK2^{L83V/H84D}$. Each mutant was coexpressed with CIV1, and subsequently purified as a fully activated cyclin-bound heterodimeric complex, under conditions essentially

† Structures have been deposited in the PDB, ID codes: 2iw6, 2iw8, 2iw9.

* To whom correspondence should be addressed. E-mail martin.noble@biop.ox.ac.uk; Tel. +44 (0)1865 275373; Fax. +44 (0)1865 275182.

‡ Laboratory of Molecular Biology, Oxford.

⊥ Northern Institute for Cancer Research, Newcastle.

§ AstraZeneca, Macclesfield.

△ Present address: MRC-LMB, Hills Road, Cambridge, CB2 2QH, UK.

[a] Abbreviations. CDK, cyclin-dependent kinase; $CDK2^{F82H}$, mutant of CDK2 with F82H; $CDK2^{L83V/H84D}$, mutant of CDK2 with L83V and H84D; $CDK2^{F82H/L83V/H84D}$, mutant of CDK2 with F82H, L83V and H84D; $CDK2^{K89T}$, mutant of CDK2 with K89T; $CDK2^{F82H/L83V/H84D/K89T}$, mutant of CDK2 with F82H, L83V, H84D and K89T; cycA3, human cyclin A fragment, with residues 174−432; GST, glutathione S-transferase; GSH, glutathione; pRB, retinoblastoma protein; RMSD, root-mean-squared deviation.)

10.1021/jm060216x CCC: $33.50
Published on Web 08/12/2006

```
CDK2  ---------MENFQKV EKIGEGTYG VV YKARNKLTG-EVV ALK KIRLDTET---EGVPST  47
CDK4  -------MATSRYEPV AEIGVGAYG TV YKARDPHSG-HFV ALK SVRVPNGGGGGGGLPIS  52

CDK2  AIR EISLLKELN---HPNI VKLLDVIHT-----ENKLYLV FEFLHQD LKK FMDASALTGI  99
CDK4  TVR EVALLRRLEAFEHPNV VRLMDVCATSRTDREIKVTLV FEHVDQD LRT YLDKAPPPGL  112

CDK2  PLPLIKSYLFQLLQGLAFCHSHRVLHR DLK PQNLL INTEGAIKL ADFGL ARAFGVPVRTY  159
CDK4  PAETIKDLMRQFLRGLDFLHANCIVHR DLK PENIL VTSGGTVKL ADFGL ARIYSYQM-AL  171

CDK2  THEVVTLWYRAPEILLGCKYYSTAVDIWSLGCIFAEMVTRRALFPGDSEIDQLFRIFRTL  219
CDK4  TPVVVTLWYRAPEVLLQS-TYATPVDMWSVGCIFAEMFRRKPLFCGNSEADQLGKIFDLI  230

CDK2  GTPDEVVWPGVTSMPDYKPSFPKWARQDFSKVVPPLDEDGRSLLSQMLHYDPNKRISAKA  279
CDK4  GLPPEDDWPRDVSLP--RGAFPPRGPRPVQSVVPEMEESGAQLLLEMLTFNPHKRISAFR  288

CDK2  ALAHPFFQDVTKPVPHLRL                                          298
CDK4  ALQHSYLHKDEGNPE----                                          303
```

Figure 1. Sequence alignment of CDK2 and CDK4. The sequence alignment of human CDK2 and CDK4 is shown, based on a multiple sequence alignment of multiple CDKs. Residues shown in bold are those in CDK2 that contact one or more CDK2 ligands and the equivalent residues in CDK4.

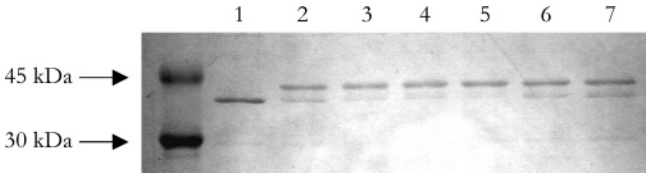

Figure 2. Phosphorylation of the retinoblastoma protein by wild-type and mutant CDK2/cycA3. The assay was carried out as described in materials and methods. The proteins used were: Lane 1, no kinase; Lane 2, wild-type CDK2/cycA3; Lane 3, CDK2$^{F82H/L83V/H84D}$/cycA3; Lane 4, CDK2^{K89T}/cycA3; Lane 5, CDK2$^{F82H/L83V/H84D/K89T}$/cycA3; Lane 6, CDK2^{F82H}/cycA3; Lane 7, CDK2^{L83VH84D}/cycA3.

identical to those of wild-type CDK2. All mutants retained kinase activity against a fragment of the retinoblastoma protein, an endogenous substrate of CDK2 (Figure 2).

The roles of the four residues in inhibitor selectivity were assayed using the 300-fold CDK2-selective 6-cyclohexylmethoxy-2-(4′-sulfamoylanilino)purine compound **1** (NU6102[18]) and the 26-fold CDK4-selective ((2-chloro-5-methyl-phenyl)-{6-[4-(3-(dimethylamino)-2-hydroxy-propoxy)-phenylamino]-pyrimidin-4-yl}-amino)-acetonitrile compound **2** (Figure 3; Table 1). IC_{50} values of compound **1** were determined against all five CDK2 mutants. The IC_{50} of compound **1** against wild-type CDK2 was also measured as a control and matched the published values.[18] IC_{50} values of compound **2** against CDK2^{K89T}, CDK2$^{F82H/L83V/H84D}$, CDK2$^{F82H/L83V/H84D/K89T}$, and wild-type CDK2 were also determined (Table 1). The relative activity of each of the CDK2 mutants with respect to wild-type CDK2 was also determined by comparison of the DMSO-only control reactions (Table 2).

Effects of Residue Changes on CDK2 Structure and on Inhibitor Potency. Compound **2** is a member of a family of CDK4-selective bisanilinopyrimidines.[36,37] Cocrystal structures of five analogues bound to wild-type CDK2 show the aminopropoxy moiety projecting out of the ATP binding site, and interacting with Lys89. The potency of compound **2** against CDK2^{K89T} (0.14 μM) is 18 times greater than against wild-type CDK2 (2.6 μM) and is only 3-fold less than against wild-type CDK4 (0.047 μM). The potency of compound **2** against

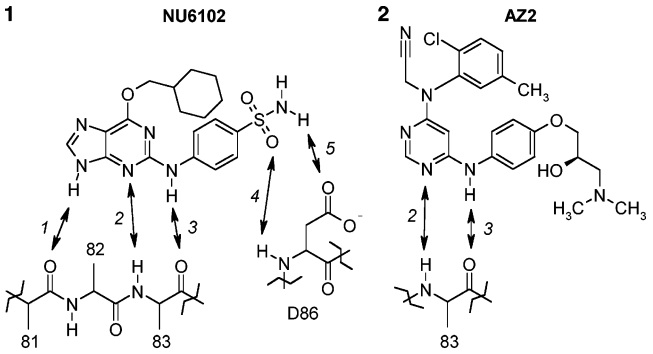

Structure	Hydrogen-bond length (Å)				
	1	*2*	*3*	*4*	*5*
CDK2 / NU6102	2.8	3.4	2.8	3.1	3.0
CDK2^{K89T} / NU6102	2.7	3.3	2.8	3.5	2.8
CDK2$^{F82H/L83V/H84D}$ / NU6102	2.8	3.4	2.8	3.0	3.0
CDK2^{K89T} / AZ2	n/a	3.1	2.8	n/a	n/a

Figure 3. The structural formulas of compound **1** (NU6102[18]) and compound **2** are shown. Hydrogen bonds formed between the inhibitors and the kinase residues are indicated by numbered double-headed arrows, with the bond lengths tabulated.

CDK2$^{F82H/L83V/H84D}$ (7.3 μM) is 3-fold lower than its potency against wild-type CDK2 (2.6 μM), while its potency against CDK2 $^{F82H/L83V/H84D/K89T}$ (0.64 μM) is approximately 4-fold more than its potency against wild-type wild-type CDK2. Thus, when presented in the context of CDK2, the CDK4 residues H82/V83/D84 appear to decrease the relative of affinity of the kinase for compound **2**, while the residue T89 appears to promote the relative affinity.

The cocrystal structure of compound **2** bound to CDK2^{K89T}/cycA3 was solved. The structure of the kinase is overall very similar to that of compound **1**/CDK2/cycA3 (CDK2 Cα RMSD = 0.34 Å) (Figure 4A). Compound **2** binds to the ATP binding site in a similar conformation to those of the five analogous compounds bound to monomeric wild-type CDK2.[36,37] Two hydrogen bonds are formed between the inhibitor and the main-chain atoms of Leu83, analogous to those seen in the majority of CDK2/ligand crystal structures.[11] Activation of CDK2 by

Table 1. IC_{50} Values and 95% Confidence Intervals for Binding of Inhibitors to CDK2 and Mutant CDK2s

	compound **1**			compound **2**		
protein	IC_{50} (nM)	$CI_{0.95}$ (nM)	relative IC_{50}	IC_{50} (μM)	$CI_{0.95}$ (μM)	relative IC_{50}[d]
CDK2	8.1	7.0−9.4	1	2.6	2.0−3.4	55
$CDK2^{K89T}$	8.9	7.6−10	1	0.14	0.12−0.17	3
$CDK2^{L83V/H84D}$	21	19−23	3	n/d[a]	n/d	n/d
$CDK2^{F82H}$	33	28−39	4	n/d	n/d	n/d
$CDK2^{F82H/L83V/H84D}$	103	85−126	13	7.3	5.3−9.9	155
$CDK2^{F82H/L83V/H84D/K89T}$	120	86−160	15	0.64	0.47−0.87	14
CDK4[b]	1600	1000[c]	200	0.047	0.021[c]	1

[a] n/d = not determined. [b] Reference 18; P. Jewsbury, personal communication. [c] Standard deviation. [d] Relative IC_{50} values given here are calculated from data presented in this table: values for selectivity stated in the Introduction are from measurements reported in the literature and differ somewhat from these values.

Table 2. Relative Kinase Activities and Standard Deviation of the Mutant CDK2s

protein	relative activity
CDK2	1
$CDK2^{K89T}$	1.03 ± 0.18
$CDK2^{F82H}$	0.76 ± 0.15
$CDK2^{L83V/H84D}$	1.05 ± 0.18
$CDK2^{F82H/L83V/H84D}$	0.38 ± 0.16
$CDK2^{F82H/L83V/H84D/K89T}$	0.38 ± 0.02

phosphorylation of Thr160 and binding to cycA3 leads to conformation changes in and around the ATP ribose/phosphate binding site.[20] These conformation changes appear to affect the binding of nitrile moieties in this compound series. The nitrile moiety of compound **2** bound to the activated $CDK2^{K89T}$ forms water-mediated hydrogen bonds to the side-chain of Glu51 and the main chain nitrogen of Asp145 and Phe146. The structure of an analogous compound bound to monomeric wild-type CDK2 (compound **17**[36]) shows polar contacts from the nitrile to the main-chain nitrogen atom and side-chain carboxylate group of Asp145.

Substitution of Lys89 for Thr causes the side chain of Asp86 to reorient and form a hydrogen bond with the Thr89 side-chain.

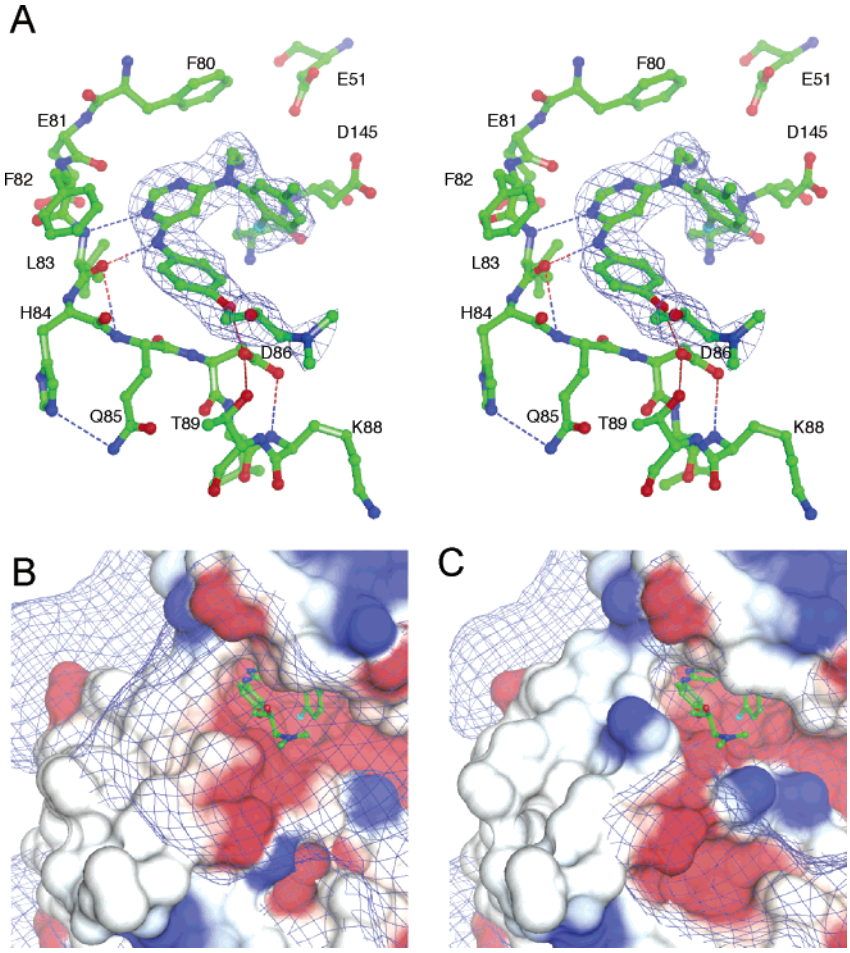

Figure 4. Compound **2** bound to the ATP binding site of $CDK2^{K89T}$. A (stereo): Selected residues of CDK2 are shown, with carbon, nitrogen, and oxygen atoms colored green, blue, and red, respectively. Compound **2** is drawn in a similar style. For clarity, only one stereoisomer is shown. The blue grid represents the REFMAC5 weighted $2F_o - F_c$ electron density map of the final refined structure. The map is contoured at 0.21 electrons/Å^3, or 1.0 times the RMSD of the map. Hydrogen bonds are depicted by dotted lines (B,C): The electrostatic potential of $CDK2^{K89T}$ (Panel B) is compared with the electrostatic potential of wild type CDK2 (Panel C). Electrostatics were calculated in CCP4MG by a finite difference Poisson-Boltzmann method[42] and are used to color the solvent-accessible surface of the two proteins, such that positive potential is blue and negative potential red. The mesh is a contour of the potential field at −0.01 V and defines the volume in which significant favourable interactions are made with a positively charged group.

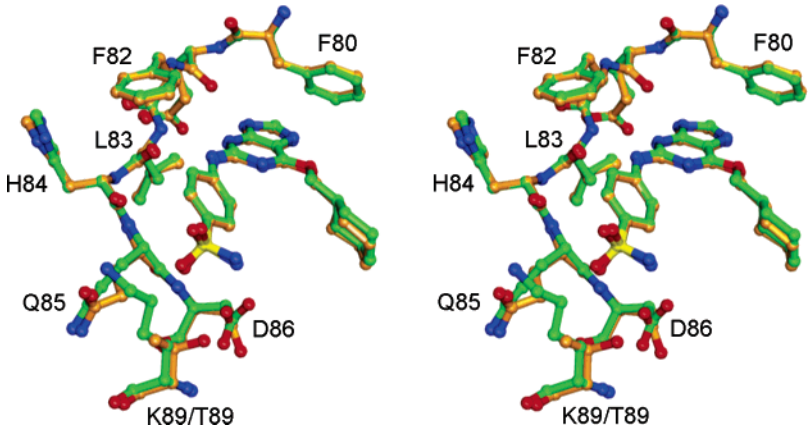

Figure 5. (Stereo) Comparison of the binding of compound **1** to wild-type CDK2 and CDK2^{K89T}. Residues of CDK2 and compound **1** from the compound **1**/CDK2/cycA3 crystal structure are shown with carbon, nitrogen, oxygen, and sulfur atoms coloured green, blue, red, and yellow, respectively. Residues of CDK2^{K89T} and compound **1** from the compound **1**/CDK2^{K89T}/cycA3 crystal structure shown in a similar style, with carbon atoms colored orange.

The electron density for the structure of compound **2** bound to CDK2^{K89T}/cycA3 allows a confident fitting of one of the isomers of the aminopropoxy moiety of the inhibitor, in contrast to the structures of compound **2** analogues bound to wild-type CDK2. The moiety is seen to project out of the kinase active site, forming van der Waals interactions with the side chain of Thr89. A lysine side chain would be expected to clash with the inhibitor in this conformation. The Lys89Thr mutation also has a significant effect on the electrostatic potential of this region of the kinase. In the compound **2**/CDK2^{K89T}/cycA3 structure, the amine moiety of the inhibitor, which is expected to be positively charged at physiological pH ($pK_a \approx 9.8$), binds within the −0.01 V potential field contour, implying favorable binding (Figure 4B). In contrast, the amine lies outside the field in a model of compound **2** bound to wild-type CDK2. The 18-fold increase in potency of compound **2** against CDK2^{K89T} therefore seems to be due to a more favorable steric and electrostatic binding environment for the aminopropoxy moiety in CDK2^{K89T}, compared to that in wild-type CDK2.

Other CDK inhibitors exploit the K89T residue difference, both by chance and by design. For example, the CINK4 inhibitor is a >33-fold selective CDK4 inhibitor (1.5 μM) over CDK2 (>50 μM).[13] A homology model of CDK4, with CINK4 bound in the active site, shows a benzyl moiety projecting toward the Thr102 residue, the equivalent CDK4 residue to CDK2 Lys89. It is predicted that the additional bulk of the Lys89 side-chain inhibits binding of CINK4 in CDK2. A diarylurea series of CDK4 inhibitors were designed to exploit three poorly conserved CDK4 residues, including Thr102.[14,38] The crystal structure of one such compound (compound II; an inhibitor of CDK4 with an IC_{50} of 210 nM), bound to mutated CDK2 (bearing, among others, K89T), shows a cyclic amine moiety interacting with the Thr89 side-chain.[39] Again it is predicted that a lysine side chain would inhibit the compound binding to CDK2. CDK inhibitors also exploit attractive interactions to the Lys89 side-chain. Purvalanol B is a >1500-fold selective CDK2 inhibitor (6 nM) over CDK4 (>10 μM). The crystal structure of Purvalanol B bound to CDK2 shows an attractive charge−charge interaction between the amine of Lys89 and the carboxylic acid of the inhibitor.[19]

Compound **1** is a potent and specific member of the O^6-alkylguanine CDK2 inhibitor family (Table 1[18]). The Lys89/Thr102 sequence difference was targeted in the structure-aided design of compound **1**. Compared with the phenolic analogue (compound **25**, 69 nM[40]), the sulfonamide moiety increased the potency for CDK2, and selectivity over CDK4, by factors of 100 and 50, respectively. However, the structure of compound **1**/CDK2/cycA3 shows that the sulfonamide forms two hydrogen bonds to Asp86, which is conserved in CDK4, and forms van der Waals contacts with the Lys89 side-chain.[18] Here, we show that the K89T mutation makes no significant difference to the potency of compound **1** (8.9 nM) compared to against wild-type CDK2 (8.1 nM). In contrast, the potency of compound **1** is decreased 13-fold against CDK2$^{F82H/L83V/H84D}$ (103 nM). Further introduction of the K89T mutation does not further significantly alter compound **1** potency (CDK2$^{F82H/L83V/H84D/K89T}$, 120 nM). Dissection of the roles of the individual members of the triplet of mutations show that compound **1** potency decreased 4- and 3-fold for the mutants CDK2^{F82H} (33 nM) and CDK2$^{L83V/H84D}$ (21 nM). It therefore seems that the three mutations F82H, L83V, and H84D act together in decreasing the potency of compound **1**, while K89T has no significant role. As with the changes in compound **2** potency by the HVD mutations, the effect on ATP binding may play a role (see below).

The structures of compound **1** bound to CDK2^{K89T}/cycA3 (Figure 5; CDK2 Cα RMSD = 0.32 Å) and CDK2$^{F82H/L83V/H84D}$/cycA3 (Figure 6; CDK2 Cα RMSD = 0.31 Å) were solved. The inhibitor binds in a similar conformation to both CDK2s in a similar conformation to that seen in the wild-type CDK2/cycA3 structure.[18] As seen in the compound **2**/CDK2^{K89T}/cycA3 structure, the Chi2 angle of the Asp86 residue in the compound **1**/CDK2^{K89T}/cycA3 structure differs from that seen in the wild-type structure by ∼60°, which permits the formation of a hydrogen-bond with the side-chain of Thr89. As this residue is conserved in CDK4, it is reasonable to expect that compound **1** interacts with CDK4 in a similar manner in this region. This rotation leads to a decrease in the length of the hydrogen bond between the inhibitor and the Asp86 side-chain (Figure 3). In contrast, the hydrogen bond to the Asp86 backbone nitrogen is lengthened due to a rotation by 11° of the sulfonamide relative to the aryl ring. The similar potency of compound **1** against wild-type CDK2/cycA3 and CDK2^{K89T}/cycA3 implies that the changes to the hydrogen-bond geometries compensate for each other.

The structure of compound **1**/CDK2$^{F82H/L83V/H84D}$/cycA3 shows that the substitution of the three CDK2 residues with the equivalent CDK4 residues makes little overall difference to the structure of the kinase, or the binding geometry of the inhibitor. The backbone of the kinase is not significantly altered,

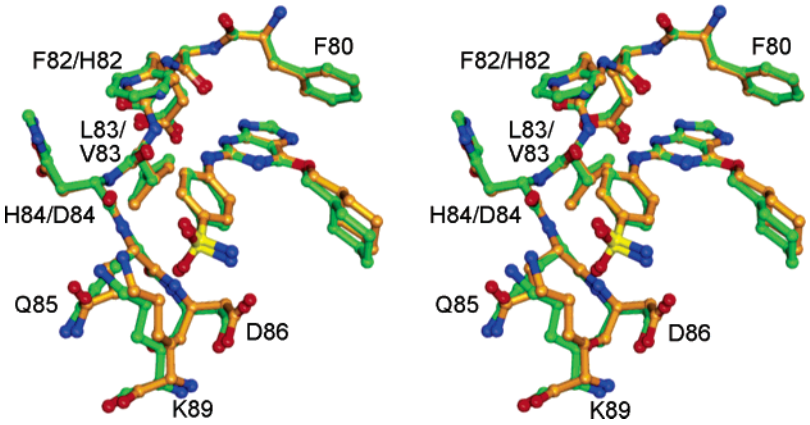

Figure 6. (Stereo) Comparison of the binding of compound **1** to wild-type CDK2 and CDK2$^{F82H/L83V/H84D}$. Residues of CDK2 and compound **1** from the compound **1**/CDK2/cycA3 crystal structure are shown with carbon, nitrogen, oxygen, and sulfur atoms coloured green, blue, red, and yellow, respectively. Residues of CDK2$^{F82H/L83V/H84D}$ and compound **1** from the compound **1**/CDK2$^{F82H/L83V/H84D}$/cycA3 crystal structure are shown in a similar style, with carbon atoms colored orange.

the conformation of the side-chains are equivalent, and the geometry of the three hydrogen-bonds formed between the inhibitor guanine moiety and the kinase are not significantly altered (Figure 3). In a manner analogous to compound **1** binding to wild-type CDK2, the side chains of His82 and Val83 of CDK2$^{F82H/L83V/H84D}$ make van der Waals contacts with the inhibitor, while the side-chain of Asp84 projects away from compound **1**, making no direct contact.

The greater impact that F82H has on compound **1** potency, compared to that of L83V and H84D combined, may be due to the more significant change in the chemical identity of the side-chains in F82H compared to L83V. The phenyl ring of Phe82 and the imidazole ring of His82 are both aromatic and could potentially form $\pi-\pi$ interactions with the purine ring of compound **1**. However, the His82 imidazole ring is expected to be basic (p$K_a \approx 6.7$) and may therefore have a delocalized positive charge around the ring. In contrast, the L83 and V83 side-chains only differ by a methylene unit. Although residue 82 is remote from the site of phosphotransfer, proteins that carry the F82H mutation have significantly decreased relative kinase activity (Table 2), presumably due to a decreased affinity for ATP.

A second possible explanation of the marked effect of the F82H mutant comes from a consideration of "second shell" residues, i.e., amino acid residues that do not contact ATP or inhibitors directly, but that are in contact with residues that do. While, in general, the contribution of such residues to selectivity is likely to be smaller than that of directly contacting residues, they might be expected to have an effect on the conformation and mobility of the first shell residues, such as F82, that have been targeted in this study. Notably, F82 contacts V29 in CDK2, a residue that is replaced by a phenylalanine (F31) in CDK4. The aromatic character of F31 in CDK4, in particular, suggests that it may well contribute to stabilizing an appropriate stacking conformation for the interaction between the hinge residue and any ATP-site directed ligand. Hence the mutation F82H, in the absence of the corresponding mutation V29F, may produce a structure, and a corresponding composite molecular field, that is not fully representative of CDK4 in this region. A combinatorial mutation of all first and second shell residues is beyond the scope of this paper, but may be required to realize the full potential of mutagenesis in dissecting inhibitor specificity.

While this work confirms some predictions made about the causes of inhibitor selectivity, notably the role of K89T in CDK4-inhibitor selectivity, some apparent anomalies remain. More potent members of the bisanilinopyrimidine family have been described as deriving selectivity from interactions with residues conserved between CDK2 and CDK4, most prominently Phe80/93.[36,37] Similarly, NU6094, the des-sulfonamide analogue of compound **1**, shows only 16-fold selectivity for CDK2 over CDK4, implying that the interactions of the sulfonamide group with the conserved residue Asp86 contribute to inhibitor selectivity as well as potency.[18] In both cases, the most obvious explanation is that there are local structural differences in the two kinases that lead to the differential interaction with these conserved residues. The conformational perturbation of Asp86 as a consequence of mutation of Lys89 to a Thr may exemplify such structural differences. The effect of this conformational difference is neutral on the binding of compound **1**, presumably because of compensatory changes in the strengths of the two hydrogen bonds formed between the sulfonamide and Asp86. The compound **1** phenolic-analogue, in contrast, forms different interactions with the Asp86/Lys89 pair and may even bind more strongly to the conformation of Asp86 observed in CDK4. Further mutagenesis of CDK2 is required to address such subtleties of inhibitor binding.

Conclusions

The four nonconserved CDK2/CDK4 residues tested here (F82/H95, L83/V96, H84/D97, and K89/T102) all play a role in CDK inhibitor selectivity. The K89T mutation causes significant changes to the electrostatic and steric local environment of the kinase. These changes are well exploited by compound **2**. However, the potency of compound **1** is unaffected by this mutation, implying further potency and/or selectivity may still be derived by targeting this residue.

Mutagenesis of the other three residues to those of CDK4, causes a decrease in potency of compound **1** and compound **2**. This apparent differential binding of the purine/pyrimidine of compound **1**/compound **2**, respectively, corroborates one of the conclusions of a recent study of kinase inhibitor selectivities.[41] The inhibition profiles of 20 clinically relevant kinase inhibitors were assessed against 119 kinases. The study showed that chemically similar compounds can have very different selectivity profiles and therefore that the general chemical scaffold of an inhibitor class does not dictate specificity. That compound **2** appears to be making weaker interactions with the three CDK4 residues His95/Val96/Asp87 compared with the CDK2 Phe82/Leu83/His84, implying that further CDK4 selectivity may be achievable by replacing the pyrimidine core. It should be noted,

Table 3. Data Collection and Refinement Statistics

	compound **1**/CDK2^{K89T}/cycA3	compound **1**/CDK2$^{F82H/L83V/H84D}$/cycA3	compound **2**/CDK2^{K89T}/cycA3
PDB accession code	2i	EBI-14659	EB-14660
		Data Collection	
space group	$P2_12_12_1$	$P2_12_12_1$	$P2_12_12_1$
unit cell *a*, *b*, *c* (Å)	73.76, 134.10, 148.12	73.89, 135.32, 148.32	73.66, 133.89, 148.28
maximal resolution (Å)	2.00	2.30	2.30
highest resolution shell	2.10−2.00	2.41−2.30	2.41−2.30
observations	256673	165025	224073
unique reflections	97458	64531	61358
completeness (%)[a]	98.1 (96.7)	97.1 (94.4)	93.8 (87.0)
R_{merge}[a,b]	0.062 (0.354)	0.128 (0.315)	0.102 (0.439)
mean $I/\sigma I$[a]	6.0 (1.4)	3.6 (2.3)	5.5 (1.4)
multiplicity[a]	2.6 (2.5)	2.6 (2.5)	3.7 (2.2)
		Refinement	
protein atoms	8701	8650	8877
inhibitor atoms	56	56	72
residues modeled	A0-A37	A0-A297	A-2-A37
	A42-A297	B176−B282	A41−296
	B178−B282	B285−B432	B176−B432
	B285−B432	C0−C220	C0−C295
	C0−C220	C252−C296	D178-D432
	C251−C296	D178-D432	
	D178-D432		
nonprotein monomers modeled	2 × compound **1**	2 × compound **1**	2 × compound **2**
	2 × MTG	2 × MTG	2 × MTG
	2 × Mg^{2+}	1 × Mg^{2+}	1 × Mg^{2+}
	384 waters	309 waters	114 waters
resolution range	47.14−2.00	65.94−2.30	41.17−2.30
R_{conv}[c] (%)	0.210	0.212	0.228
R_{free}[d] (%)	0.240	0.254	0.287
most favored geometry[e]	92.1%	91.3%	88.1%
RMSD bond (Å)	0.012	0.012	0.018
RMSD angle (deg)	1.294	1.409	1.713
mean B-factor (Å^2)			
protein	36.3	14.4	45.3
ligand	38.2	9.7	58.8
solvent	39.4	15.1	45.3

[a] Figures in brackets are those for the highest resolution shell only. [b] $R_{merge} = \Sigma_h\Sigma_j|I_{h,j} - \bar{I}|/\Sigma_h\Sigma_j|I_{h,j}|$, where $I_{h,j}$ is the jth observation of reflection h. [c] $R_{conv} = \Sigma_h||F_o| - |F_c||/\Sigma_h|F_o|$, where F_o and F_c are the observed and calculated structure factor amplitudes respectively for the reflection h. [d] R_{free} is equivalent to R_{conv} calculated from the 5% subset of reflections not used in refinement. [e] Residues lying in the most favored regions of the Ramachandran plot, as assessed by PROCHECK.[43]

however, that this might have a significant impact on the geometry of the attached groups, which in and of themselves have important roles in potency and selectivity.

Designing potent and specific kinase inhibitors remains a challenging task, but should be helped by the increasingly detailed understanding of inhibitor/kinase interactions, such as that provided by this study.

Experimental Section

Ligand Contacting Residues. Ligand/CDK2 interactions were calculated using CONTACT,[15] using a distance cutoff of 5 Å. The following structures were used: 1HCK (ATP/CDK2[16]), 1JST (ATP/CDK2/cycA3[17]), 1H1S (compound **1**/CDK2/cycA3[18]), 1CKP (purvalanol B/CDK2[19]), 1E9H (indirubin-5-sulfonate/CDK2/cycA3[20]), 1DM2 (hymenialdisine/CDK2[21]), 1FVT and 1FVV (oxindole **3**/CDK2 and oxindole **4**/CDK2/cycA3[22]), 1DI8 (quinazoline **2**/CDK2[23]) and 1AQ1 (staurosporine/CDK2[24]).

Sequence Alignment. The protein sequences of human CDK2 (Swiss-Prot accession code P24921), CDK4 (P11802), and CDK6 (Q00532) were used as search sequences against the nrdb95 database[25] using BLAST2.[26] A multiple sequence alignment was generated using the BLOSUM30 matrix and ClustalW with default settings.[27] The alignment of CDK2 and CDK4 was then extracted.

Mutagenesis of CDK2. Site-directed mutagenesis was performed using pUC18-CDK2 as a template, and the Fisher method.[28] Primers were designed (Tables S1 and S2) to produce the following CDK2 mutants: CDK2^{F82H}, CDK2$^{L83V/H84D}$, CDK2$^{F82H/L83V/H84D}$, CDK2^{K89T}, and CDK2$^{F82H/L83V/H84D/K89T}$. Mutated CDK2 sequences were subcloned into an expression vector for expression of GST-tagged CDK2, phosphorylated on Thr160.[29] Clones were verified by restriction-enzyme digestion and DNA sequencing.

Protein Expression and Purification. Wild-type CDK2 and the five mutant CDK2 proteins were expressed and purified in a fully active form (bound to a cyclin A fragment and phosphorylated on Thr160) as previously described.[29] Briefly, a modified pGEX-6P-1 vector was used to coexpress GST-tagged CDK2 and a monomeric CDK-activating kinase (CIV1), which phosphorylated CDK2 on Thr160 in vivo in *E. coli*. A fragment of cyclin A (residues 174−432, cycA3) was separately expressed in *E. coli*. The GST-CDK2 lysate was bound to GSH-sepharose beads (Amersham), and the cycA3 lysate was then applied. GST-CDK2/cycA3 was eluted with reduced glutathione (Sigma), and the GST tag was removed by 3C protease digestion. CDK2/cycA3 was purified to homogeneity by gel filtration and checked by mass spectrometry.

Phosphorylation of pRB. Five nanograms of wild-type and each mutant CDK2/cycA3 was separately added to 1 μg of a GST-tagged C-terminal fragment of pRb (residues 792−928; a gift from N. Brown) in buffer R (50 mM Tris/HCl, pH 7.4, 10 mM $MgCl_2$, 1 mM ATP, 1 mM DTT) in a final volume of 10 μL and incubated for 30 min at 21 °C. The reactions were terminated by addition of 10 μL SDS−PAGE loading dye and heating to 100 °C for 5 min. The reactions were analyzed by SDS−PAGE.

Inhibition Assays. IC_{50} values were measured using a modification of a CDK1/cyclin B1 inhibition assay.[30] Wild-type or mutant CDK2/cycA3 (1.7 nM in 10 mM Tris, pH 7.5, 80 mM NaCl, 20% glycerol) was incubated with histone H1 (type III-S, Sigma, Gillingham, UK; 0.83 mg/mL) and 12.5 μM ATP (Sigma) in buffer K (50 mM Tris/HCl, pH 7.5, 5 mM $MgCl_2$) supplemented with [^{32}P-γ]-ATP (5.7 kBq/reaction; ICN, Irvine, CA) and 1% DMSO

(v/v). Inhibitors, made up in 100% DMSO, were added to final concentrations in the range 0.3 nM to 30 μM to the reaction mix to give a final volume of 30 μL, and reactions were then incubated for 10 min at 30 °C. Each inhibitor concentration was assayed in duplicate in the same experiment. DMSO-only controls were included in each experiment. A wild-type CDK2/cycA3 control was included in each set of reactions, and each experiment was repeated twice. Reactions were terminated by spotting onto phosphocellulose filter paper (Whatman P81, Maidstone, UK), drying for 20 s, and then washing (five times for 5 min each) in 1% (v/v) phosphoric acid (Riedel de-Haën; Honeywell, Seelze, Germany). The filter papers were then air-dried overnight. ^{32}P incorporation into histone H1 was measured by using a Phospho-Image plate (Molecular Dynamics, Model SO230; Amersham Biosciences, Uppsala, Sweden) read on an FLA3000 plate reader (FujiFilm, Hemel Hempsted, UK), and the resulting images were analyzed using ImageGauge (FujiFilm) and ImageJ (NIH, Bethesda, MD). Image plate response was calibrated by comparison to the measured response due to spotted amounts of [^{32}P-γ]-ATP of known radioactivity. IC_{50} values and 95% confidence intervals ($CI_{0.95}$) were determined by least-squares fitting of the data to the Hill equation (Prism version 3.03; Graphpad Software, CA).

X-ray Diffraction Data Collection and Processing. Inhibitor/CDK2/cycA3 crystals were grown in potassium chloride and ammonium sulfate as described,[20] and cryo-protected by brief immersion in 6−8 M sodium formate, before flash freezing at 100 K. Data were collected using a MarCCD (compound **2**/CDK2^{K89T}/cycA3) and an ADSC Q4 CCD (compound **1**/CDK2^{K89T}/cycA3 and compound **1**/CDK2$^{F82H/L83V/H84D}$/cycA3) at the ESRF, France. Data were processed using MOSFLM,[31] SCALA,[32] and the CCP4 suite.[15]

Structure Solution and Refinement. All structures were solved by molecular replacement, using the protein chains of the compound **1**/CDK2/cycA3 complex as a search model (1H1S;[18]), modified in silico to replace the mutated residues with alanines. Models were subjected to rigid body refinement, followed by TLS and individual atomic refinement using REFMAC5.[33] Ligand models were created using the Monomer Library Sketcher.[15] Model rebuilding and refinement was carried out using O[34] and REFMAC5.[33] Water molecules were added using the CCP4 implementation of ARP/wARP[35] and verified by manual inspection. Data collection, processing, and refinement statistics are shown in Table 3. The model of compound **2** bound to wild-type CDK2/cycA3 was created by performing an all-CDK2 Cα alignment between the compound **2**/CDK2^{K89T}/cycA3 structure and the compound **1**/CDK2/cycA3 structure (1H1S), removing the coordinates of compound **1**, and adding the transformed coordinates of compound **2** to the CDK2/cycA3 structure.

Acknowledgment. We thank Tim Hunt for the human CDK2 and cyclin A constructs, and Herbie Newell and Roger Griffin for use of their facilities and many enlightening discussions. We are grateful to the beam-line scientists at the ESRF for providing excellent facilities during data collection. We thank Irene Taylor and Jenny Gibson for laboratory support, Neil Oldham for mass spectrometry facilities, and Ed Lowe for assistance with data collection. This research was supported by grants from the BBSRC and AstraZeneca Plc, UK.

Supporting Information Available: Primer sequences for CDK2 mutagenesis. This material is available free of charge via the Internet at http://pubs.acs.org.

References

(1) Sherr, C. J. Cancer cell cycles. *Science* **1996**, *274*, (5293)), 1672−1677.
(2) Malumbers, M.; Carnero, A. Cell cycle deregulation: a common motif in cancer. In *Progress in Cell Cycle Research*; Meijer, L.; Jézéquel, A., Roberge, M., Eds.; 2003; Vol. 5, pp 5−18.
(3) Swanton, C. Cell-cycle targeted therapies. *Lancet Oncol.* **2004**, *5*, (1), 27−36.
(4) Donnellan, R.; Chetty, R. Cyclin D1 and human neoplasia. *Mol. Pathol.* **1998**, *51*, (1)), 1−7.
(5) Ruas, M.; Peters, G. The p16INK4a/CDKN2A tumor suppressor and its relatives. *Biochim. Biophys. Acta* **1998**, *1378*, (2)), F115−77.
(6) Morgan, D. O. Cyclin-dependent kinases: Engines, Clocks and Microprocessors. *Annu. Rev. Cell Dev. Biol.* **1997**, *13*, 261−291.
(7) Catzavelos, C.; Bhattacharya, N.; Ung, Y. C.; Wilson, J. A.; Roncari, L.; Sandhu, C.; Shaw, P.; Yeger, H.; Morava-Protzner, I.; Kapusta, L.; Franssen, E.; Pritchard, K. I.; Slingerland, J. M. Decreased levels of the cell-cycle inhibitor p27Kip1 protein: prognostic implications in primary breast cancer. *Nat. Med.* **1997**, *3* (2), 227−230.
(8) Porter, P. L.; Malone, K. E.; Heagerty, P. J.; Alexander, G. M.; Gatti, L. A.; Firpo, E. J.; Daling, J. R.; Roberts, J. M. Expression of cell-cycle regulators p27Kip1 and cyclin E, alone and in combination, correlate with survival in young breast cancer patients. *Nat. Med.* **1997**, *3*, (2), 222−225.
(9) Keyomarsi, K.; Tucker, S. L.; Buchholz, T. A.; Callister, M.; Ding, Y.; Hortobagyi, G. N.; Bedrosian, I.; Knickerbocker, C.; Toyofuku, W.; Lowe, M.; Herliczek, T. W.; Bacus, S. S. Cyclin E and survival in patients with breast cancer *N. Engl. J. Med.* **2002**, *347* (20), 1566−1575.
(10) Pagano, M.; Tam, S. W.; Theodoras, A. M.; Beer-Romero, P.; Del Sal, G.; Chau, V.; Yew, P. R.; Draetta, G. F.; Rolfe, M. Role of the ubiquitin-proteasome pathway in regulating abundance of the cyclin-dependent kinase inhibitor p27. *Science* **1995**, *269* (5224), 682−685.
(11) Hardcastle, I.-R.; Golding, B.-T.; Griffin, R.-J. Designing inhibitors of cyclin-dependent kinases. *Annu. Rev. Pharmacol. Toxicol.* **2002**, *42*, 325−348.
(12) Barvian, M.; Boschelli, D. H.; Cossrow, J.; Dobrusin, E.; Fattaey, A.; Fritsch, A.; Fry, D.; Harvey, P.; Keller, P.; Garrett, M.; La, F.; Leopold, W.; McNamara, D.; Quin, M.; Trumpp-Kallmeyer, S.; Toogood, P.; Wu, Z.; Zhang, E. Pyrido[2,3-*d*]pyrimidin-7-one inhibitors of cyclin-dependent kinases. *J. Med. Chem.* **2000**, *43* (24), 4606−4616.
(13) Soni, R.; Muller, L.; Furet, P.; Schoepfer, J.; Stephan, C.; Zumstein-Mecker, S.; Fretz, H.; Chaudhuri, B. Inhibition of cyclin-dependent kinase 4 (Cdk4) by fascaplysin, a marine natural product. *Biochem. Biophys. Res. Commun.* **2000**, *275*, (3)), 877−884.
(14) Honma, T.; Hayashi, K.; Aoyama, T.; Hashimoto, N.; Machida, T.; Fukasawa, K.; Iwama, T.; Ikeura, C.; Ikuta, M.; Suzuki-Takahashi, I.; Iwasawa, Y.; Hayama, T.; Nishimura, S.; Morishima, H. Structure-based generation of a new class of potent Cdk4 inhibitors: new de novo design strategy and library design. *J. Med. Chem.* **2001**, *44*, (26)), 4615−4627.
(15) CCP4. The CCP4 suite: programs for protein crystallography. *Acta Crystallogr. D* **1994**, *50*, 760−763.
(16) De Bondt, H. L.; Rosenblatt, J.; Jancarik, J.; Jones, H. D.; Morgan, D. O.; Kim, S.-H. Crystal structure of cyclin-dependent kinase 2. *Nature* **1993**, *363*, 595−602.
(17) Russo, A. A.; Jeffrey, P. D.; Pavletich, N. P. Structural basis of cyclin-dependent kinase activation by phosphorylation. *Nat. Struct. Biol.* **1996**, *3* (8), 696−700.
(18) Davies, T.-G.; Bentley, J.; Arris, C.-E.; Boyle, F. T.; Curtin, N.-J.; Endicott, J.-A.; Gibson, A.-E.; Golding, B.-T.; Griffin, R.-J.; Hardcastle, I.-R.; Jewsbury, P.; Johnson, L.-N.; Mesguiche, V.; Newell, D.-R.; Noble, M.-E. M.; Tucker, J.-A.; Wang, L.; Whitfield, H.-J. Structure-based design of a potent purine-based cyclin-dependent kinase inhibitor. *Nat. Struct. Biol.* **2002**, *9* (10), 745−749.
(19) Gray, N. S.; Wodicka, L.; Thunnissen, A. M.; Norman, T. C.; Kwon, S.; Espinoza, F. H.; Morgan, D. O.; Barnes, G.; LeClerc, S.; Meijer, L.; Kim, S. H.; Lockhart, D. J.; Schultz, P. G. Exploiting chemical libraries, structure, and genomics in the search for kinase inhibitors. *Science* **1998**, *281* (5376), 533−538.
(20) Davies, T. G.; Tunnah, P.; Meijer, L.; Marko, D.; Eisenbrand, G.; Endicott, J. A.; Noble, M. E. Inhibitor binding to active and inactive CDK2: the crystal structure of CDK2-cyclin A/indirubin-5-sulphonate. *Structure (Camb)* **2001**, *9* (5), 389−397.
(21) Meijer, L.; Thunnissen, A. M.; White, A. W.; Garnier, M.; Nikolic, M.; Tsai, L. H.; Walter, J.; Cleverley, K. E.; Salinas, P. C.; Wu, Y. Z.; Biernat, J.; Mandelkow, E. M.; Kim, S. H.; Pettit, G. R. Inhibition of cyclin-dependent kinases, GSK-3beta and CK1 by hymenialdisine, a marine sponge constituent. *Chem. Biol.* **2000**, *7* (1), 51−63.
(22) Davis, S. T.; Benson, B. G.; Bramson, H. N.; Chapman, D. E.; Dickerson, S. H.; Dold, K. M.; Eberwein, D. J.; Edelstein, M.; Frye, S. V.; Gampe, R. T., Jr.; Griffin, R. J.; Harris, P. A.; Hassell, A. M.; Holmes, W. D.; Hunter, R. N.; Knick, V. B.; Lackey, K.; Lovejoy, B.; Luzzio, M. J.; Murray, D.; Parker, P.; Rocque, W. J.; Shewchuk, L.; Veal, J. M.; Walker, D. H.; Kuyper, L. F. Prevention of chemotherapy-induced alopecia in rats by CDK inhibitors. *Science* **2001**, *291* (5501), 134−137.

(23) Shewchuk, L.; Hassell, A.; Wisely, B.; Rocque, W.; Holmes, W.; Veal, J.; Kuyper, L. F. Binding mode of the 4-anilinoquinazoline class of protein kinase inhibitor: X-ray crystallographic studies of 4-anilinoquinazolines bound to cyclin-dependent kinase 2 and p38 kinase. *J. Med. Chem.* **2000**, *43* (1), 133−138.
(24) Lawrie, A. M.; Noble, M. E. M.; Tunnah, P. R.; Brown, N. R.; Johnson, L. N.; Endicott, J. A. Protein kinase inhibition by staurosporine: details of the molecular interaction determined by X-ray crystallographic analysis of a CDK2-staurosporine complex. *Nat. Struct. Biol.* **1997**, *4*, 796−801.
(25) Holm, L.; Sander, C. Removing near-neighbour redundancy from large protein sequence collections. *Bioinformatics* **1998**, *14* (5), 423−429.
(26) Altschul, S. F.; Gish, W.; Miller, W.; Myers, E. W.; Lipman, D. J. Basic local alignment search tool. *J. Mol. Biol.* **1990**, *215*, (3), 403−410.
(27) Thompson, J. D.; Higgins, D. G.; Gibson, T. J. CLUSTAL W: improving the sensitivity of progressive multiple sequence alignment through sequence weighting, position-specific gap penalties and weight matrix choice. *Nucleic Acids Res.* **1994**, *22* (22), 4673−4680.
(28) Fisher, C. L.; Pei, G. K. Modification of a PCR Based Site-Directed Mutagenesis Method. *BioTechniques* **1997**, *23*, 570−574.
(29) Brown, N. R.; Noble, M. E. M.; Endicott, J. E.; Johnson, L. N. The structural basis for specificity of substrate and recruitment peptides for cyclin-dependent kinases. *Nat. Cell Biol*. **1999**, *1* (7), 438−443.
(30) Vesely, J.; Havlicek, L.; Strnad, M.; Blow, J. J.; Donella-Deana, A.; Pinna, L.; Letham, D. S.; Kato, J.-Y.; Detivaud, L.; Leclerc, S.; Meijer, L. Inhibition of cyclin-dependent kinases by purine analogues. *Eur. J. Biochem*. **1994**, *224*, 771−786.
(31) Leslie, A. G. W. Recent changes to the MOSFLM package for processing film and image plate data Joint CCP4 and ESF-EAMCB. *Newsl. Protein Crystallogr*. **1992**, 26.
(32) Evans, P. R. Data Reduction; Science and Engineering Research Council UK: Daresbury Laboratory, Warrington, 1993; pp 114−122.
(33) Murshudov, G. N.; Vagin, A. A.; Dodson, E. J. Refinement of macromolecular structures by the maximum-liklihood method. *Acta Crystallogr. D* **1997**, *53*, 240−255.
(34) Jones, T. A.; Zou, J. Y.; Cowan, S. W.; Kjeldgaard. Improved methods for binding protein models in electron density maps and the location of errors in these models. *Acta Crystallogr A* **1991**, *47* (2), 110−119.
(35) Perrakis, A.; Morris, R.; Lamzin, V. S. Automated protein model building combined with iterative structure refinement. *Nat. Struct. Biol.* **1999**, *6* (5), 458−463.
(36) Beattie, J. F.; Breault, G. A.; Ellston, R. P.; Green, S.; Jewsbury, P. J.; Midgley, C. J.; Naven, R. T.; Minshull, C. A.; Pauptit, R. A.; Tucker, J. A.; Pease, J. E. Cyclin-dependent kinase 4 inhibitors as a treatment for cancer. Part 1: identification and optimisation of substituted 4,6-Bis anilino pyrimidines. *Bioorg. Med. Chem. Lett.* **2003**, *13* (18), 2955−2960.
(37) Breault, G. A.; Ellston, R. P.; Green, S.; James, S. R.; Jewsbury, P. J.; Midgley, C. J.; Pauptit, R. A.; Minshull, C. A.; Tucker, J. A.; Pease, J. E. Cyclin-dependent kinase 4 inhibitors as a treatment for cancer. Part 2: identification and optimisation of substituted 2,4-bis anilino pyrimidines. *Bioorg. Med. Chem. Lett.* **2003**, *13* (18), 2961−2966.
(38) Honma, T.; Yoshizumi, T.; Hashimoto, N.; Hayashi, K.; Kawanishi, N.; Fukasawa, K.; Takaki, T.; Ikeura, C.; Ikuta, M.; Suzuki-Takahashi, I.; Hayama, T.; Nishimura, S.; Morishima, H. A novel approach for the development of selective Cdk4 inhibitors: library design based on locations of Cdk4 specific amino acid residues. *J. Med. Chem.* **2001**, *44* (26), 4628−4640.
(39) Ikuta, M.; Kamata, K.; Fukasawa, K.; Honma, T.; Machida, T.; Hirai, H.; Suzuki-Takahashi, I.; Hayama, T.; Nishimura, S. Crystallographic approach to identification of cyclin-dependent kinase 4 (CDK4)-specific inhibitors by using CDK4 mimic CDK2 protein. *J. Biol. Chem.* **2001**, *276* (29), 27548−2754.
(40) Hardcastle, I. R.; Arris, C. E.; Bentley, J.; Boyle, F. T.; Chen, Y.; Curtin, N. J.; Endicott, J. A.; Gibson, A. E.; Golding, B. T.; Griffin, R. J.; Jewsbury, P.; Menyerol, J.; Mesguiche, V.; Newell, D. R.; Noble, M. E.; Pratt, D. J.; Wang, L. Z.; Whitfield, H. J. N2-substituted O6-cyclohexylmethylguanine derivatives: potent inhibitors of cyclin-dependent kinases 1 and 2. *J. Med. Chem.* **2004**, *47* (15), 3710−3722.
(41) Fabian, M. A.; Biggs, W. H., 3rd; Treiber, D. K.; Atteridge, C. E.; Azimioara, M. D.; Benedetti, M. G.; Carter, T. A.; Ciceri, P.; Edeen, P. T.; Floyd, M.; Ford, J. M.; Galvin, M.; Gerlach, J. L.; Grotzfeld, R. M.; Herrgard, S.; Insko, D. E.; Insko, M. A.; Lai, A. G.; Lelias, J. M.; Mehta, S. A.; Milanov, Z. V.; Velasco, A. M.; Wodicka, L. M.; Patel, H. K.; Zarrinkar, P. P.; Lockhart, D. J. A small molecule-kinase interaction map for clinical kinase inhibitors. *Nat. Biotechnol.* **2005**, *23* (3), 329−336.
(42) Potterton, L.; McNicholas, S.; Krissinel, E.; Gruber, J.; Cowtan, K.; Emsley, P.; Murshudov, G. N.; Cohen, S.; Perrakis, A.; Noble, M. Developments in the CCP4 molecular-graphics project. *Acta Crystallogr. D Biol. Crystallogr.* **2004**, *60* (Pt 12, Pt 1), 2288−2294.
(43) Laskowski, R. A.; MacArthur, M. W.; Moss, D. S.; Thornton, J. M. PROCHECK: a program to check the stereochemical quality of protein structures. *J. Appl. Crystallogr*. **1993**, *26*, 283−291.

JM060216X